

# Magnetic properties of ultrahigh-pressure eclogites controlled by retrograde metamorphism: A case study from the ZK703 drillhole in Donghai, eastern China

Qingsheng Liu<sup>a,\*</sup>, Qingsong Liu<sup>b</sup>, Zeming Zhang<sup>c</sup>, Haijun Xu<sup>d</sup>,  
Lungsang Chan<sup>e</sup>, Tao Yang<sup>a</sup>, Zhenmin Jin<sup>d</sup>

<sup>a</sup> Department of Geophysics, China University of Geosciences, Wuhan 430074, China

<sup>b</sup> National Oceanography Centre, University of Southampton, European Way, Southampton SO14 3ZH, UK

<sup>c</sup> Institute of Geology, CAGS, Beijing 100037, China

<sup>d</sup> Faculty of Earth Sciences, China University of Geosciences, Wuhan 430074, China

<sup>e</sup> Department of Earth Sciences, University of Hong Kong, Pokfulam Road, Hong Kong, China

Received 14 February 2006; received in revised form 6 October 2006; accepted 11 October 2006

## Abstract

Parallel studies on rock magnetic properties, petrology and mineralogy were conducted on 16 eclogite samples from the ZK703 hole and magnetic susceptibilities and densities of 41 eclogite samples with different degree of retrograde metamorphism (from fresh eclogite to fully-retrograded eclogite) from the Chinese Continental Scientific Drilling (CCSD) near the ZK703 hole, located at Donghai, southern Sulu ultrahigh-pressure metamorphic belt, eastern China. Results show: (1) that the high-field slopes obtained from the hysteresis loops (the paramagnetic fraction  $\chi_{\text{para}}$ ) and density have a positive correlation with the volume concentration of garnet + omphacite, a typical mineral assemblage used to semi-quantify the degree of retrograde metamorphism. The low-field slopes obtained from hysteresis loops (the ferrimagnetic susceptibility fraction  $\chi_{\text{ferri}}$ ), saturation isothermal remanent magnetization  $M_{\text{rs}}$  and saturation magnetization  $M_{\text{s}}$  have a positive correlation with the volume concentration of symplectite, a mineral related to retrograded metamorphism. Therefore they could be potential indicators for quickly semi-quantifying the degree of retrograde metamorphism of the eclogite units. (2) The dominant magnetic carriers in retrograded eclogites are magnetite particles in pseudo-single domain grain size region. (3) The  $P$ – $T$  conditions during the retrograde (decompressional) process could first increase the concentration of magnetite, which can reach up to 3% for extensively retrograded eclogite and then was dissolved for fully-retrograded eclogite. Therefore, change in the magnetite contents during the retrograde process is the major factor controlling the magnetism of retrograde eclogites.

© 2006 Published by Elsevier B.V.

**Keywords:** Rock magnetism; Retrograde metamorphism; Ultrahigh-pressure eclogite; Sulu orogen

## 1. Introduction

Satellite magnetic data has demonstrated that there exist some broad relationships between large-scale geologic/tectonic features and satellite-altitude magnetic fields (Langel and Hinze, 1998; Pikington and Percival,

\* Corresponding author. Tel.: +86 27 87481462;  
fax: +86 27 67883251.

E-mail address: [lqs321@cug.edu.cn](mailto:lqs321@cug.edu.cn) (Q. Liu).

2001). Further quantitative interpretations of aeromagnetic and MAGSAT anomalies with long-wavelength suggested that the lower crust also acquire significant magnetizations (Toft and Haggerty, 1988; Fountain et al., 1992; Wasilewski and Mayhew, 1992; Pechersky and Genshaft, 2002). However, the accurate knowledge of magnetic mineralogy, magnetic petrology and the redox state in the Earth's crust is still very fragmentary.

So far, several mechanisms about the origin of the magnetization in the deep crust have been put forward, including, thermal viscous remanent magnetization (TVRM), Hopkinson effect, metamorphism (Schlinger, 1985; Liu and Gao, 1992; Kelso et al., 1993; Liu et al., 2000), remanent magnetization of rocks with hematite–ilmenite solid solution (HISS) at all crustal levels (Kletetschka et al., 2002), and lamellae magnetism in the hematite–ilmenite series (McEnroe et al., 2001; Robinson et al., 2002; Kasama et al., 2003, 2004; Dyar et al., 2004; McEnroe et al., 2004; Robinson et al., 2004).

To cast more constraints on the mechanism for the magnetization of the lower crust, rock magnetic studies on eclogite units are important. This also has further important significances for geodynamics. For example, Boundy et al. (1992) proposed a tectonic origin of the fabrics and implications for deep crustal deformation processes by structural development and petrofabrics of eclogite facies shear zones, Bergen Arcs, western Norway.

The eclogite units at the Dabie-Sulu ultrahigh-pressure (UHP) metamorphic belt have important information for the dynamics of plate tectonic processes at convergent margins (Liou and Zhang, 1996; Ye et al., 1996). These rocks were metamorphosed at depths of 50–150 km and rapidly exhumed to the surface (Xu et al., 1992; Cong and Wang, 1994; Cong et al., 1994). The various types of eclogites in this region have experienced different degrees of retrograde metamorphism (Zhang et al., 2000).

Even though extensive studies (geology, petrology, mineralogy, geochemistry, geochronology and geophysics) have been conducted on the Dabie-Sulu UHP belt and the retrograde eclogites, little is known about its magnetic properties and its magnetic mineralogy, especially the corresponding effects of retrograde metamorphism.

In this study, 57 samples of variously retrograded eclogites were collected from both the ZK 703 drill and the Chinese Continental Scientific Drilling (CCSD) main hole at Donghai region, eastern China. Petrophysical parameters including densities of all samples and

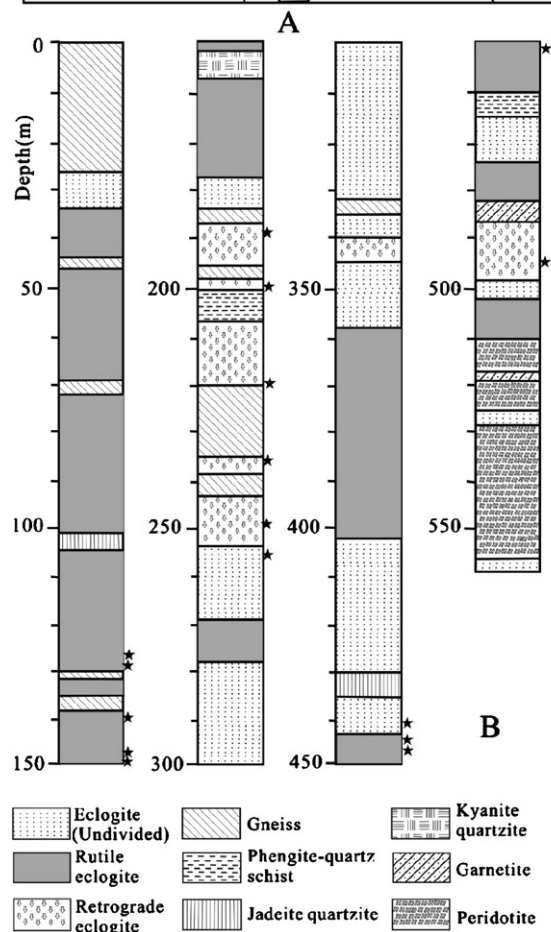
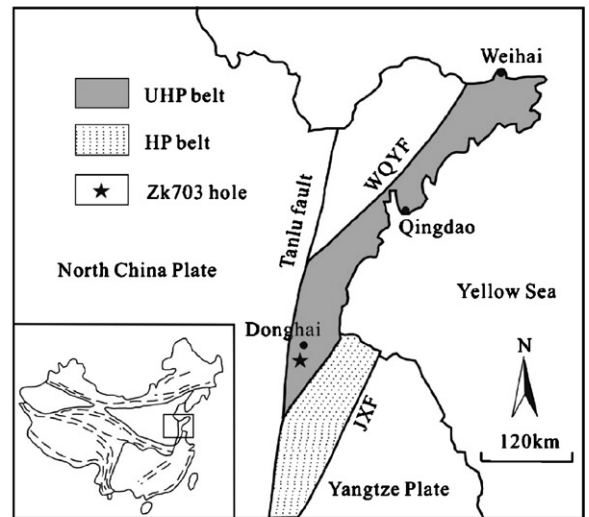


Fig. 1. Location of the Sulu UHP metamorphic belt (A) and lithological profile of the ZK703 drillhole (B). Stars in (B) mark the location of the samples examined in this study.

magnetic parameters of hysteresis loops of 16 samples in ZK703 hole and magnetic susceptibilities of 41 samples from CCSD main hole were conducted. The Donghai UPH minerals have experienced decompressional breakdown reactions, the secondary minerals occurring as symplectites or symplectic coronas, commonly with a multilayer structure. Mineral paragenesis showed that the eclogites have been subjected to two stages of retrograde recrystallization, amphibolite facies, followed by greenschist facies metamorphism (Zhang et al., 2000). Therefore, these samples are ideal for testing whether there is a relationship between the magnetic properties and the retrograde metamorphic degree. We will finally try to propose some rock magnetic parameters as potentially efficient means for a high-resolution and fast survey of large numbers of samples.

## 2. Geological setting and sampling

The Sulu UHP metamorphic belt is located between the Wulian-Qingdao-Yantai fault on the northwest and Jiashan-Xiangshui fault on the south in eastern China (Fig. 1A). The UHP belt consists not only of the primary UHP metamorphic eclogites, but also of amphibolite-facies rocks and upper greenschist-facies retrograded rocks from eclogite-facies rocks (Wang et al., 2000). The Donghai ZK703 drillhole (34°25'N/118°40'E, ~558 m in depth) lies in the south of the Sulu UHP metamorphic belt. Eclogites represent about 55% (~300 m in thickness) in thickness of the whole drillhole (Fig. 1B). They are interwinded with many thin layers of biotite gneiss, phengite-quartz schist, jadeite quartzite and kyanite quartzite. A detailed description of the lithology and petrology is given by Zhang et al. (2000) (Fig. 1B).

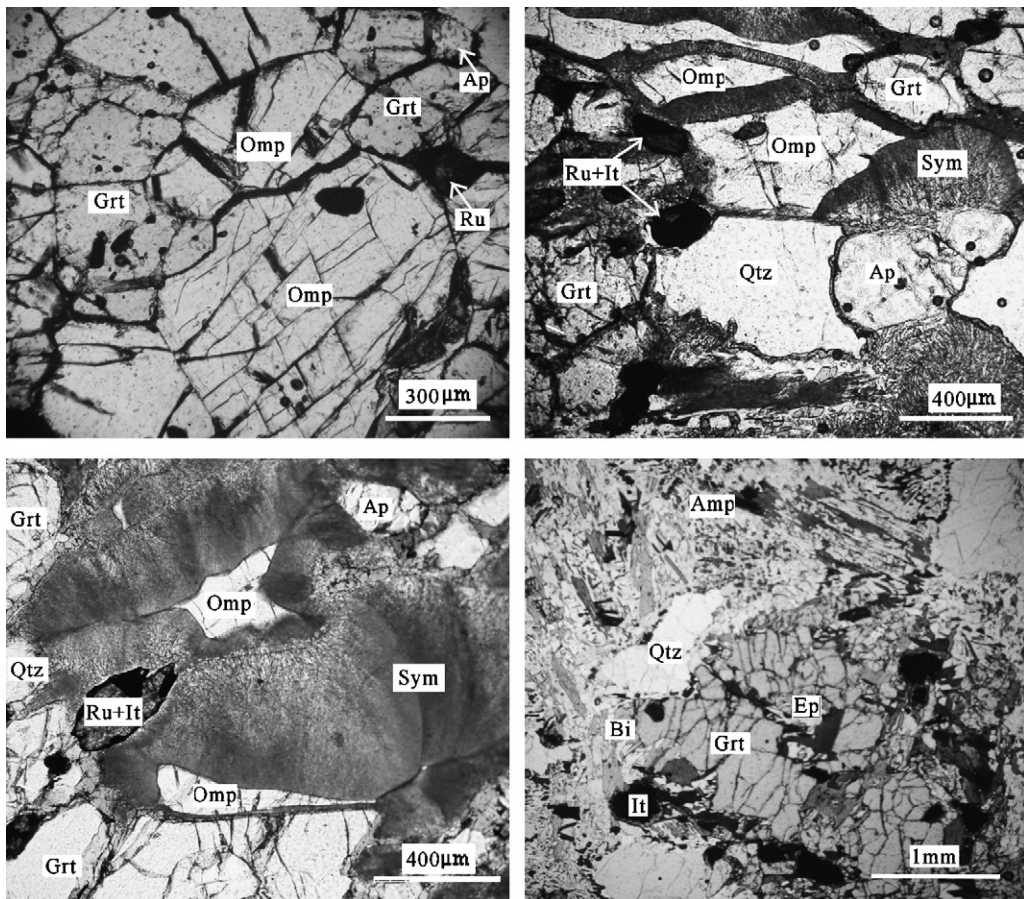


Fig. 2. Microphotographs of UHP metamorphic eclogites, showing increasing degree of retrogression. Sample 11 (upper left) and sample 14 (upper right) is slightly retrograded eclogite. Sample 30 (lower left) is extensively retrograded eclogite with omphacites replaced by symplectites. Sample 51 (lower right) eclogite which has been transformed partly to epidote amphibolite. Grt: garnet; Omp: omphacite; Ru: rutile; Il: ilmenite; Sym: symplectite; Ap: apatite; Qtz: quartz; Bi: biotite; Ep: epidote; Amp: amphibole.

Nine types of rocks have been identified (Fig. 1B), including eclogite (undivided), rutile eclogite, retrograde eclogite, gneiss, phengite-quartz schist, jadeite quartzite, kyanite quartzite, garnetite and peridotite. To address effects of retrograde process on the magnetic properties of eclogite, constrained by petrologic studies, 16 fresh samples of different retrograde metamorphic degrees were collected from the drillhole (Fig. 2). Surface weathering has little effect on these samples (Zhang et al., 2000). Among them, nine samples have experienced retrograde metamorphism. More specifically, sample 11 (129 m) and sample 14 (148 m) are located within rutile eclogite. Sample 32 (257 m) and sample 51 (443 m) belong to undivided eclogite. The others are recognized as retrograde eclogite.

In addition, in order to make up insufficiency of samples in the ZK703 hole, densities and magnetic susceptibilities of 41 samples with different retrograded eclogites (raw eclogites, slight and moderate retrograded eclogites, extensive retrograded eclogites and full retrograded eclogites) from CCSD main hole near to the ZK703 hole were measured.

### 3. Experimental methods

#### 3.1. Compositional analysis

Compositional analyses for major minerals were determined with a JEOL superprobe 733 using a wavelength dispersive system at the Analytical Center of China University of Geosciences (Wuhan). The experimental conditions were 15 kV acceleration potential and 20 nA beam current.

#### 3.2. Rock magnetic experiments

Low-field magnetic susceptibilities ( $\chi$ ) of the samples were measured with a Kappa Bridge (KLY-2) at room temperature. The temperature-dependence of  $\chi$  was also measured using the Kappa Bridge, equipped with a CS-2 furnace, from room temperature to 700 °C, in an Argon environment with steps of 5 °C.

Hysteresis loops were measured on an automated Princeton Measurements Vibrating Sample Magnetometer (VSM Model 2900). The maximum field was 1 T. Hysteretic parameters (saturation magnetization,  $M_s$ , saturation isothermal remanent magnetization,  $M_{rs}$ , coercivity,  $B_c$ ) were calculated after subtracting the paramagnetic contribution ( $\chi_{para}$ , the high-field

slope). The coercivity of remanence ( $B_{cr}$ ) was determined by the backward DC demagnetization of  $M_{rs}$ . Contributions from ferrimagnetic minerals ( $\chi_{ferri}$ ) to the bulk magnetic susceptibility (e.g., magnetite and maghemite) are calculated by  $\chi - \chi_{para}$ . The ratio  $\chi_{ferri}/\chi_{para}$  is used to quantify the relative contributions of the ferrimagnetic and paramagnetic fractions to  $\chi$ .

Day plot was constructed to estimate the grain-sizes of magnetic minerals (Day et al., 1977; Dunlop, 2002) (Fig. 4). Low temperature measurements of samples were performed with a Quantum Design Susceptometer (MPMS). A 2 T saturation isothermal remanent magnetization (SIRM) was acquired at 20 K, and then heated up to 300 K in zero fields with a temperature error  $\pm 1$  K (the curve is referred as to LT-SIRM).

Anhyseretic remanent magnetization (ARM) was imparted in a 200 mT alternating field with a superimposed 50  $\mu$ T direct bias field using a Dtech D2000 instrument. ARM is then expressed as  $\chi_{arm}$ , after normalizing by the 50  $\mu$ T direct bias fields. A more detailed description of the application of these rock magnetic proxies is summarized in Section 5.2.

### 4. Results

#### 4.1. Photography

The microstructure studies on four representative samples are illustrated in Fig. 2. Sample 11 underwent only slight retrograde metamorphism. It consists of garnet, omphacite, apatite and minor rutile. The concentration of garnet + omphacite is up to 70% and omphacites are rimmed by thin symplectic coronas of amphibole and albite. Sample 14 has undergone an intermediate degree of retrograde metamorphism, containing garnet, omphacite and quartz. Omphacites have been partly replaced by symplectic corona of amphibole + albite, and garnets by corona of amphibole and/or biotite. For the extensively retrograde eclogite (sample 30), omphacites are partly or completely replaced by symplectites of amphibole and albite, garnets partly by coronas of amphibole, and rutile by ilmenite. For sample 51, content of garnet + omphacite is only 10%, it has been transformed to garnet amphibolite. Amphibole + plagioclase occur as symplectite after omphacites, garnets are rimmed by symplectic corona of biotite and plagioclase, rutile by ilmenite. The exact volume concentrations of the garnet + omphacite and symplectite are summarized in Table 1.

Table 1  
Summary of magnetic and major mineral assemblages of eclogites from the ZK703 hole<sup>a</sup>

Sample	Lithology	$\rho$	$\chi$	$\chi_{\text{arm}}$	$B_c$	$B_{\text{cr}}$	$M_{\text{rs}}$	$M_s$	$\chi_{\text{ferri}}$	$\chi_{\text{para}}$	$B_{\text{cr}}/B_c$	$M_{\text{rs}}/M_s$	Grt (%)	Omp (%)	Grt+Omp (%)	Sym (%)
11	RE	3.46	3.645	2.544	6.31	14.9	0.99	9.22	0.94	2.71	2.36	0.107	41	29	70	19
14	RE	3.30	29.24	70.87	5.37	12.7	24.46	255.41	26.30	2.96	2.37	0.096	31	19	50	14
20	RE	3.28	8.146	8.715	5.19	15.4	3.57	55.79	6.08	2.07	2.97	0.064	34	11.6	46	20
22	RE	2.86	1.188	0.769	13.4	58.7	0.36	2.11	–	1.30	4.38	0.171	10	4	14	0
28	RE	3.06	4.778	6.845	4.45	12.3	23.52	381.48	2.41	2.37	2.76	0.062	26	9	35	38
30	RE	3.08	5.068	8.077	4.71	14.3	2.83	50.68	2.79	2.28	3.04	0.056	28	7	35	36
32	RE	2.99	6.27	14.92	7.99	17.7	6.63	54.64	4.57	1.70	2.22	0.121	0	0	0	59
51	RE	2.89	9.503	3.802	1.9	12.7	1.53	85.44	8.14	1.37	6.68	0.018	10	0	10	44
68	RE	3.07	3.662	11.32	16.8	29.9	2.97	12.98	1.44	2.22	1.78	0.228	22	0	22	48
Average		3.11	8.48	14.21	7.35	20.96	7.43	100.85	5.85	2.11	3.17	0.103	22.44	8.84	31.29	30.89
12	Band-eclogite	3.54	3.738	5.471	7.03	15	1.89	20.02	0.56	3.81	2.134	0.095	49	46	95	0
13	Eclogite	3.42	3.564	4.264	5.98	21.5	0.98	12.49	0.84	2.73	3.595	0.078	33	32	65	14
15	Quartzite eclogite	3.38	6.204	24.43	8.55	15.5	7.03	44.15	4.59	1.61	1.813	0.159	40	23	63	7
26	Eclogite	3.60	2.681	1.306	12.4	42.4	0.33	3.37	0.10	2.58	3.419	0.099	34	33	67	5
53	Rutile eclogite	3.54	2.987	0.307	6.6	16.6	0.1	2.98	0.07	2.92	2.515	0.034	35	37	72	0
54	Quartzite eclogite	3.54	2.683	2.01	5.93	24.9	0.18	2.69	0.45	2.23	4.199	0.068	39	30	69	7
57	Eclogite	3.66	2.876	0.367	13.2	32.3	0.15	2.64	0.09	2.78	2.447	0.056	33	34	67	0
Average		3.53	3.53	5.45	6.63	18.69	1.84	9.81	0.96	2.58	2.87	0.084	37.57	33.57	71.14	4.71

<sup>a</sup> Unit:  $\chi$ ,  $\chi_{\text{arm}}$ ,  $\chi_{\text{para}}$ , and  $\chi_{\text{ferri}}$  are in  $10^{-7} \text{ m}^3 \text{ kg}^{-1}$ ;  $M_{\text{rs}}$  and  $M_s$  are in  $10^{-6} \text{ Am}^2 \text{ kg}^{-1}$ . Density  $\rho$  is in  $\text{g/cm}^3$ .  $B_{\text{cr}}$  and  $B_c$  are in mT. Grt: garnet; Omp: omphacite; Sym: symplectite. RE represents retrograde eclogite.

Table 2  
Magnetic susceptibility and density of different retrograded eclogites from the CCSD main hole

Lithology	$\rho$ (g/cm <sup>3</sup> )			$\chi$ ( $\times 10^{-7}$ m <sup>3</sup> /kg)		
	min	max	mean	min	max	Mean
Raw eclogite (15)	3.25	3.70	3.48	0.82	17.90	4.76
Slightly-moderately retrograded eclogite (10)	3.13	3.45	3.29	3.91	13.10	7.51
Extensively retrograded eclogite (8)	2.90	3.26	3.12	9.98	51.90	28.60
Fully retrograded eclogite (8)*	2.72	3.05	2.88	0.71	10.50	3.42

Note: numbers in bracket are sample count.

\* Full retrograded eclogite has been transformed to epidote amphibolite.

#### 4.2. Magnetic, density and compositional analysis

The rock magnetic parameters and mineral analysis for the ZK703 hole are summarized in Table 1 and densities and susceptibilities of 41 samples from the CCSD main hole are shown in Table 2. The densities and magnetic properties of different eclogites in two holes differ significantly. For the ZK703 hole, the retrograde eclogites have density between 2.86 and 3.46 g/cm<sup>3</sup> with an average of 3.11 g/cm<sup>3</sup>. The corresponding  $\chi$  is between  $\sim 1.19$  and  $29.24 \times 10^{-7}$  m<sup>3</sup> kg<sup>-1</sup>. In contrast, the unretrograde samples have a relatively higher density ranging between 3.38 and 3.66 g/cm<sup>3</sup> with an

average of 3.53 g/cm<sup>3</sup>. The magnetic susceptibilities of these fresh samples have a narrower distribution between 2.68 and  $6.20 \times 10^{-7}$  m<sup>3</sup> kg<sup>-1</sup>, suggesting the occurrence of some alterations of magnetic properties through retrograde metamorphism (Table 1). Sample 11 has the highest concentration of garnet + omphacite (70%). In contrast, sample 32 is devoid of these UHP minerals. Unretrograded eclogites generally have higher concentrations of garnet + omphacite and lower symplectite than the retrograde eclogites (Table 1).

Densities and susceptibilities of 41 samples of eclogites with different retrograded metamorphic degrees from the CCSD are shown in Table 2. For raw eclog-

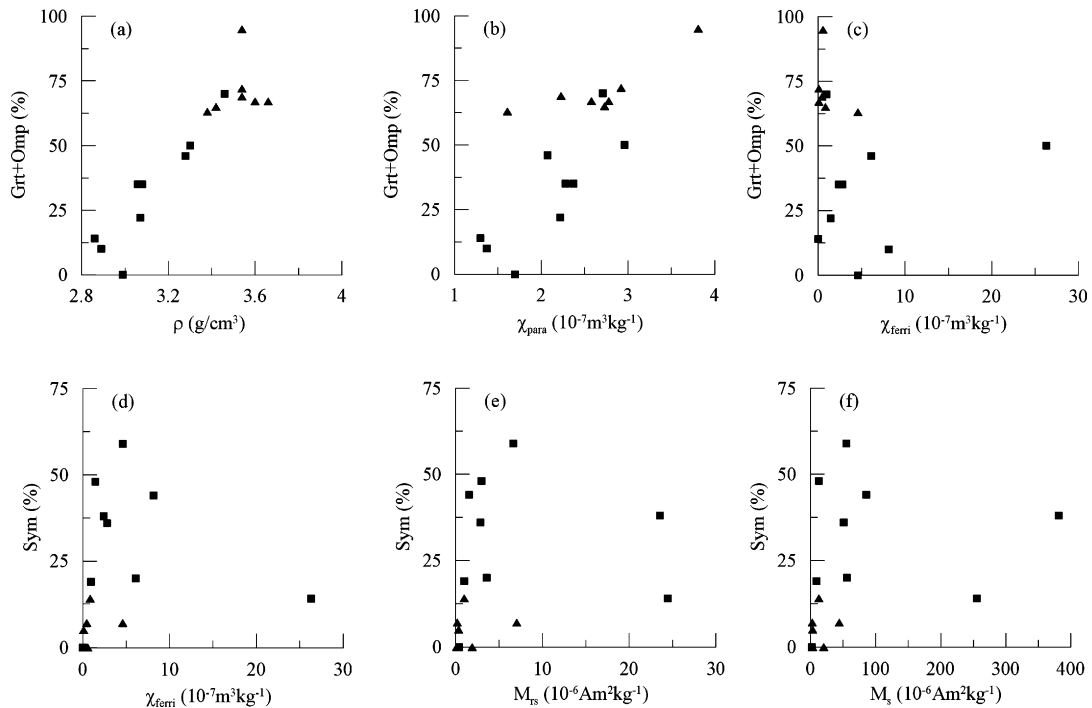


Fig. 3. Plot of density and magnetic parameters vs. concentration of garnet + omphacite and symplectite: (a)–(c) density  $\rho$ , paramagnetic susceptibility  $\chi_{\text{para}}$  and ferrimagnetic susceptibility  $\chi_{\text{ferri}}$  vs. concentration of garnet + omphacite; (d)–(f) ferrimagnetic susceptibility  $\chi_{\text{ferri}}$ , saturation isothermal remanent magnetization  $M_{\text{rs}}$  and saturation magnetization  $M_{\text{s}}$  vs. concentration of symplectite. Square and triangle represent retrograded metamorphic eclogites and raw eclogites, respectively.

Table 3  
Mineral compositions of representative eclogite samples with different retrograded metamorphic degree from CCSD main hole

Classification	No.	Mineral assemblage and content
Raw eclogite	060	Gt 50, Omp 40, Ru 4, Cc 3, Ap 2, Pr 1
	084	Gt 60, Omp 35, Ru 4, Pr 1
	121	Gt 45, Omp 40, Q 10, Ru 3, Pr 2
	332	Gt 45, Omp 40, Q 5, Ph 8, Ru 1, Pr 1
Slightly retrograded eclogite	003	Gt 45, Omp 25, Q 20, Am 4, Pl 4, Ru 1, Mt 1
	017	Gt 35, Omp 40, Q 15, Ph 2, Ru 3, Am 2, Pl 2, Mt 1
	112	Gt 50, Omp 20, Q 10, Ph 7, Ru 5, Am 2, Bi 3, Ap 1, Pr 2
	198	Gt 35, Omp 50, Q 5, Ph 3, Ru 2, Am 2, Pl 2, Mt 1
Moderately retrograded eclogite	005	Gt 25, Omp 10, Q 25, Ru 3, Am 15, Pl 20, Pr 2
	027	Gt 35, Omp 30, Q 8, Ph 4, Ru 4, Bi 3, Am 8, Pl 7, Mt 1
	071	Gt 35, Omp 25, Q 8, Ru 4, Am 12, Pl 10, Pr 2, Mt 3
	307	Gt 35, Omp 30, Q 8, Ph 6, Am 10, Pl 10, Ru 1
Extensively retrograded eclogite	030	Gt 20, Q 25, Ilm 3, Am 20, Pl 25, Bi 5, Mt 2
	058	Gt 30, Q 10, Am 20, Pl 20, Bi 8, Ilm 5, Ap 2, Ep 5
	170	Gt 50, Omp 2, Q 6, Ph 6, Ilm 2, Am 18, Pl 12, Bi 2, Mt 2
	199	Gt 25, Q 8, Ph 8, Ilm 2, Bi 2, Am 20, Pl 20, Czo 10, Mt 3
Fully retrograded eclogite	001	Gt 7, Am 35, Q 25, Pl 25, Sph 3, Bi 4, Pr 1
	006	Gt 15, Am 40, Pl 22, Bi 15, Ep 3, Sph 4, Pr 1
	035	Gt 2, Am 35, Pl 35, Bi 15, Q 5, Ep 4, Sph 4
	123	Am 58, Q 20, Bi 10, Ep 5, Pl 5, Ap 1, Sph 1

Note: Am: amphibolite; Ap: apatite; Bi: biotite; Cc: calcite; Czo: clinozoisite; Ep: epidote; Gt: garnet; Ilm: ilmenite; Mt: magnetite; Omp: omphacite; Ph: phengite; Pl: plagioclase; Pr: pyrite; Q: quartzite; Ru: rutile; Sph: titanite.

ites, slight-moderate retrograded eclogites, extensive retrograded eclogites and full retrograded eclogites, mean values of density are  $3.48 \text{ g/cm}^3$ ,  $3.26 \text{ g/cm}^3$ ,  $3.12 \text{ g/cm}^3$ , and  $2.88 \text{ g/cm}^3$ , respectively, and corresponding to susceptibilities are  $4.76 \times 10^{-7} \text{ m}^3 \text{ kg}^{-1}$ ,  $7.51 \times 10^{-7} \text{ m}^3 \text{ kg}^{-1}$ ,  $28.60 \times 10^{-7} \text{ m}^3 \text{ kg}^{-1}$  and  $3.42 \times 10^{-7} \text{ m}^3 \text{ kg}^{-1}$ , respectively (Table 2).

The relationships between magnetic parameters and garnet + omphacite and symplectite are shown in Fig. 3. Density and paramagnetic susceptibility  $\chi_{\text{para}}$  generally shows a positive correlation with the concentration (vol.%) of garnet + omphacite (Fig. 3a and b) and but low-field slope (i.e. ferrimagnetic susceptibility  $\chi_{\text{ferri}}$ ) near to be negative correlation (Fig. 3c). Symplectite is a secondary mineral related with decompressional breakdown reactions in retrograded metamorphic processes and ferrimagnetic minerals (e.g. magnetite) are generally as symplectite occurring. Therefore, the concentration of symplectite in eclogites can be used to indicate the degree of retrograde metamorphism in this region.  $\chi_{\text{ferri}}$ ,  $M_{\text{rs}}$  and  $M_{\text{s}}$  have positive correlations with symplectite contents, except for two samples with high  $M_{\text{rs}}$  and  $M_{\text{s}}$  values (Fig. 3d–f).

Domain states are related to grain-size and thus it might be possible to estimate the mean grain-size of a sample under the assumption that there is no change in magnetomineralogy. Mineralogical

analysis of representative samples with different retrograded eclogites from the CCSD is in Table 3. From slightly-moderately retrograded eclogites to extensively retrograde eclogites, the dominant magnetic mineral is magnetite (Table 3). The average grain size of magnetic minerals indicated by the Day-plot is shown in Fig. 4. Overall, magnetic minerals in both

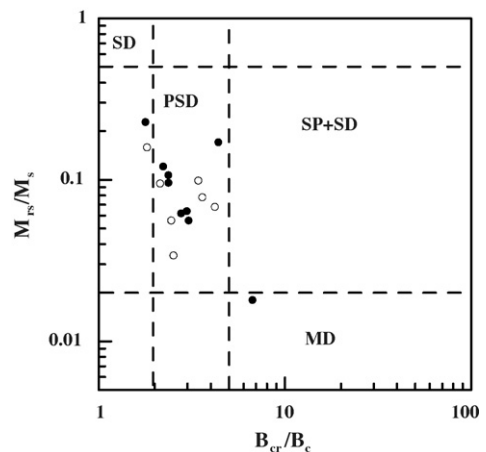


Fig. 4.  $M_{\text{rs}}/M_{\text{s}}$  and  $B_{\text{cr}}/B_{\text{c}}$  results (large solid circles) for ZK703 retrograde eclogites. The dashed areas are the data set from Day et al. (1977). The solid and open circles represent the retrograde metamorphic and raw eclogites, respectively.

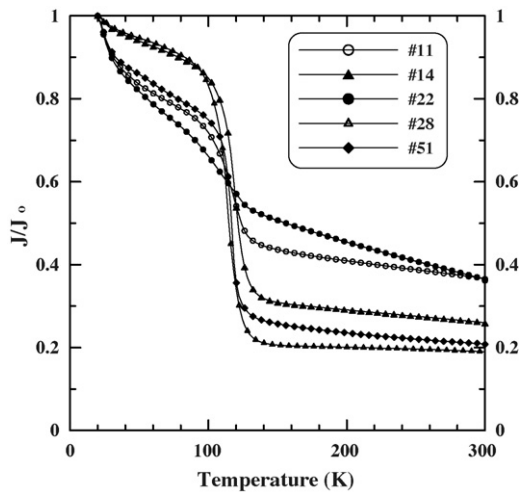


Fig. 5. Low temperature thermal demagnetization curves for representative samples.

unretrograde and retrograde eclogites are in pseudo-single domain (PSD) grain size region and overlap each other.

The low temperature heating curves are shown in Fig. 5. The remanences acquired at 20 K gradually decrease with increasing temperature. The intensity drop between 20 and 40 K could relate to pyrrhotite, but also could be caused by magnetite particles (Özdemir et al., 1993). However, its contributions to the room temperature remanence are not significant. The significant intensity drops at ~120 K indicating the presence of magnetite. Magnetite is the dominant magnetic carrier in samples, especially for samples 14, 28, and 51.

The temperature-dependence of magnetic susceptibility curves for samples 14, 30, and 51 are illustrated in Fig. 6. The distinct Curie temperatures at ~580 °C indicate that the dominant magnetic carrier is magnetite.

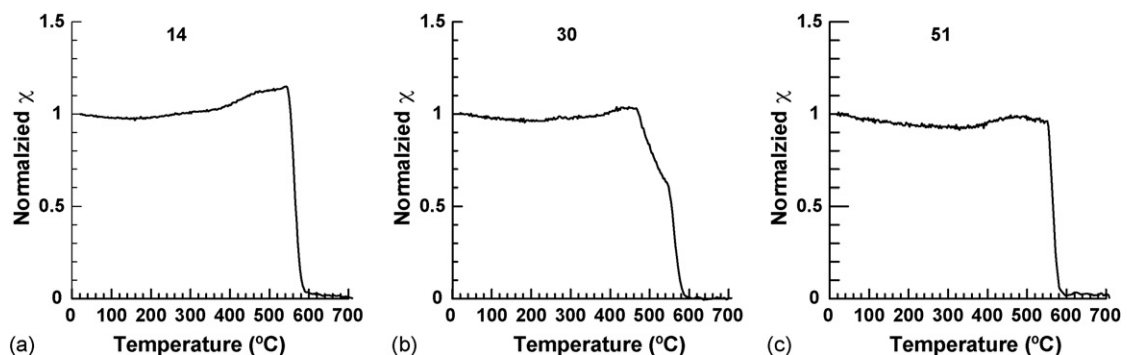


Fig. 6. Temperature-dependence of magnetic susceptibility for samples 14 (a), 30 (b) and 51 (c).

## 5. Discussion

### 5.1. Index of the retrograde metamorphic degree

The UHP eclogites of the Sulu region have experienced at least three stages of metamorphism (eclogite, amphibolite, and greenschist facies) (Zhang et al., 2000). During retrograde metamorphism from eclogite to amphibolite facies, plagioclase + biotite + amphibolite + symplectite were gradually formed by replacing garnet + omphacite + phengite. During the more advanced retrograde metamorphic stage (greenschist facies), albite + chlorite + actinolite + quartz assemblage completely replaced the primary minerals in the eclogites. Therefore, the volume concentration of garnet and omphacite decreases with increasing degrees of retrograde metamorphism. In contrast, the concentration of symplectite + amphibole will increase. Because the volume concentration of garnet + omphacite is inversely correlated to the concentration of symplectite + amphibole, in this study, we only use the volume concentration of garnet and omphacite as an index of the retrograde metamorphic degree. Table 1 reveals that the retrograde metamorphic degree of our samples is 11, 14, 28, 30, 22, and 51 in ZK703 hole. This can also be confirmed by the variations in symplectite and amphibole. For example, sample 32 has a maximum concentration (59%) of symplectite, and is totally absent of garnet + omphacite, indicating that this sample has a maximum retrograde degree. Mineral assemblage and contents of representative samples with different retrograded eclogites from CCSD show in Table 3. From raw eclogites, slight retrograded eclogites, moderate retrograded eclogites, extensive retrograded eclogites to full retrograded eclogites, contents of garnet + omphacite are from 85–90%, 70–85%,



35–65%, 25–45% to 0–15%. It indicates that from raw eclogite to full retrograded eclogite, concentration of garnet + omphacite is decreasing trend (Xu et al., 2004).

### 5.2. Interpretative framework of magnetic parameters

In this section, we will provide a framework for interpreting the magnetic parameters used in this study in terms of grain sizes and magnetic mineralogy.

SP and multi-domain (MD, >30–40  $\mu\text{m}$ ) magnetite and maghemite particles are both characterized by high susceptibility and weak remanence intensity. However, the apparent absence of SP particles in our samples can avoid such as ambiguity. Therefore, higher  $\chi/\chi_{\text{arm}}$ ,  $\chi/\text{SIRM}$ ,  $B_{\text{cr}}/B_{\text{c}}$  correspond to coarser grains. In contrast, higher ratios of  $\text{SIRM}/\chi$ ,  $\text{ARM}/\text{SIRM}$ , and  $M_{\text{rs}}/M_{\text{s}}$  indicate finer grains. For example, SD particles are expected to have the lowest  $\chi/\chi_{\text{arm}}$  ratio ( $\sim 0.09$ ) (Dankers, 1978; Maher, 1988).

The combination of  $M_{\text{rs}}/M_{\text{s}}$  and  $B_{\text{cr}}/B_{\text{c}}$  ratios is named “Day plot” (Day et al., 1977; Dunlop, 2002), which is another tool for estimating the average grain-size of magnetic minerals. Day et al. (1977) divided the Day-plot into single domain (SD,  $M_{\text{rs}}/M_{\text{s}} > 0.5$  and  $B_{\text{cr}}/B_{\text{c}} < 1.5$ ), pseudo-single domain (PSD,  $0.5 > M_{\text{rs}}/M_{\text{s}} > 0.05$  and  $4 > B_{\text{cr}}/B_{\text{c}} > 1.5$ ), and MD ( $M_{\text{rs}}/M_{\text{s}} < 0.05$  and  $B_{\text{cr}}/B_{\text{c}} > 4$ ) grain size regions. More recently, Dunlop (2002) refined these boundary values based on theoretical calculations. The newest threshold values for SD, PSD and MD particles are  $M_{\text{rs}}/M_{\text{s}} > 0.5$  and  $B_{\text{cr}}/B_{\text{c}} < 2$ ,  $0.5 > M_{\text{rs}}/M_{\text{s}} > 0.02$  and  $5 > B_{\text{cr}}/B_{\text{c}} > 2$ , and  $M_{\text{rs}}/M_{\text{s}} < 0.02$  and  $B_{\text{cr}}/B_{\text{c}} > 5$ , respectively. Based on Dunlop (2002)’s model, the Day plots of all samples are in PSD grain size region. This is further demonstrated by the interparametric ratios of  $\chi/\chi_{\text{arm}}$ , which is  $> 0.09$  for all samples.

The magnetic mineralogy can use be determined by temperature-dependence of the magnetic properties. Magnetite has a special transition point at  $\sim 120$  K ( $T_{\text{v}}$ ), where it experiences a phase transition from cubic to monoclinic  $T_{\text{v}}$  (Verwey et al., 1947; Özdemir and Dunlop, 1999; Özdemir et al., 2002). In addition, a  $\sim 580$  °C Curie temperature also can be surely assigned to nearly-stoichiometric magnetite. Figs. 5 and 6 show apparent  $\sim 120$  K  $T_{\text{v}}$  and  $\sim 580$  °C Curie temperature, indicating that the dominant magnetic carriers are magnetite. Because of the absence of SP particles, the gradually decrease of remanence intensity during heating (Fig. 5) is probably due to maghemite (Özdemir et al., 1993).

In addition, susceptibilities and densities of different retrograded eclogites from CCSD indicate in

Table 2. Densities of eclogites are decreasing with retrograded degree increasing and mean values are from  $3.48 \text{ g/cm}^3$  for raw eclogites to  $2.88 \text{ g/cm}^3$  for full retrograded eclogites. But variations of susceptibilities for different retrograded eclogites have a peak value ( $28.60 \times 10^{-7} \text{ m}^3 \text{ kg}^{-1}$ ) in extensively retrograded and it is only  $3.42 \times 10^{-7} \text{ m}^3 \text{ kg}^{-1}$  for fully retrograded eclogites (transform to epidote amphibolite) (Table 2).

### 5.3. Relationship between magnetic properties and the retrograde metamorphic degree

Zhang et al. (2000) suggested that the retrograde metamorphism at the Sulu region follows a path characterized by rapid decompression and slowly decreasing temperature. The  $P$ – $T$  conditions were around  $550$  °C and  $< 10$  kbar (Zhang et al., 1995), or alternatively  $510$ – $720$  °C and  $8$ – $12$  kbar (Enami et al., 1993). Fig. 3a and b show the relationship between concentration of garnet + omphacite and the density and paramagnetic fractions of magnetic susceptibility for the studied eclogites and results indicate that both is mostly controlled by garnet and omphacite. Compared to  $\chi_{\text{para}}$ , the concentration proxies  $\chi_{\text{ferri}}$  for ferrimagnetic minerals exhibit relative complicated patterns (Fig. 3c). Seemingly, the concentration of magnetite initially increases with decreasing Grt + Omp (vol.%) except for one sample with high susceptibility. Magnetite exists generally in symplectite as retrograded metamorphic products (Wang et al., 2000) and thus concentration of symplectite also can qualitatively study relationship between magnetic and retrograded processes. Ferrimagnetic parameters  $\chi_{\text{ferri}}$ ,  $M_{\text{rs}}$ ,  $M_{\text{s}}$  generally correlate positively with contents of symplectite except for two samples with high magnetic (Fig. 3d–f). Therefore, magnetic parameters (include paramagnetic and ferrimagnetic) can efficiently indicate retrograded metamorphic processes in this region. The formation of magnetite must relate to the replacement of the iron-bearing minerals. However, if our interpretations are correct, magnetite can be further removed when reach full retrograde metamorphic degree.

Mineral assemble of representative samples from CCSD main hole shows in Table 3. From raw eclogites to slight-moderation retrograded eclogites to extensive retrograded eclogites to full retrograded eclogites, magnetite contents corresponds to zero to 1% to 2–3% to zero. It indicates that variations of magnetite contents are increasing from unretrograded eclogites (i.e. raw eclogites) to extensively retrograded processes, and then decrease to zero when reach the fully retrograded state. Therefore, we infer that The  $P$ – $T$  conditions dur-

ing the retrograde (decompressional) process could first increase the concentration of magnetite, and then reach highest in extensive retrograded, while full retrograded process, magnetite in eclogites is dissolved. Therefore, magnetite is main factor controlling magnetic properties of various eclogites in this region.

## 6. Conclusions

Based on the discussion above, the main conclusion of this study is that magnetic properties of different retrograded eclogites are highly linked to the degree of retrograde metamorphism. From raw eclogite → slightly retrograded → moderately retrograded → extensively retrograded, ferrimagnetic susceptibility, saturation isothermal remanent magnetization and saturation magnetization generally increase, and then further decrease while reaching full retrograde eclogites. The dominant magnetic carriers are nearly stoichiometric magnetite and the overall magnetic grain size of eclogite samples are located in the PSD grain size region. SP particles are absent in our samples. The paramagnetic fractions of magnetic susceptibility are determined by the volume concentrations of garnet + omphacite resulting in a strongly positive correlation between  $\chi_{\text{para}}$  (also density) and the degree of retrograde metamorphism. Therefore,  $\chi_{\text{para}}$  and density can be efficient proxies for semi-quantitatively determining the degree of retrograde metamorphism in this region. This rock magnetic approach will be faster but non-destructive compared to the petrologic analysis especially for the preliminary survey of a long drill hole or a large amount of samples.

Finally, we revealed that the maximum concentration of magnetite occur for samples with extensive degrees of retrograde metamorphism and magnetite content is almost absent for the fully retrograded eclogites (as transform to epidote amphibolite). This could indicate that magnetite can be further dissolved by the even higher degrees of retrograde metamorphism and magnetite is a major factor controlling magnetism of retrograded eclogites. Therefore, rock magnetic methods are potentially important for evaluating the retrograde processes of eclogites in this region.

## Acknowledgements

This paper was supported by Major State Basic Research Development Program of China (“973Project” No. 2003CB716506, 2003CB716501). Q. Liu was supported by a European Commission Marie-Curie Fellowship, proposal # 7555. Low-temperature experiments

were measured at the Institute for Rock Magnetism (IRM), which is supported by the W.M. Keck Foundation, the Earth Science Division of the US National Science Foundation, and the University of Minnesota. Two anonymous reviewers provided helpful comments for improving this manuscript.

## References

- Boundy, T.M., Fountain, D.M., Austrheim, H., 1992. Structural development and petrofabrics of eclogite facies shear zones, Bergen Arcs, western Norway: implications for deep crustal deformational processes. *J. Met. Geol.* 10, 127–146.
- Cong, B., Wang, Q., 1994. Review of researches on ultrahigh-pressure metamorphic rocks in China. *Chin. Sci. Bull.* 39, 2068–2075.
- Cong, B., Wang, Q., Zhai, M., Zhao, Z., Ye, K., 1994. UHP metamorphic rocks in the Dabie-Su-Lu region, China: Their formation and exhumation. *Island Arc* 3, 135–150.
- Dankers, P.H.M., 1978. Magnetic properties of dispersed natural iron-oxides of known grain size. PhD Dissertation, University of Utrecht.
- Day, R., Fuller, M., Schmidt, V.A., 1977. Hysteresis properties of titanomagnetites: grain-size and compositional dependence. *Phys. Earth Planet. Inter.* 13, 260–266.
- Dunlop, D.J., 2002. Theory and application of the Day plot ( $M_{rs}/M_s$  versus  $H_{cr}/H_c$ ). 2. Application to data for rocks, sediments, and soils. *J. Geophys. Res.* 107 (B3), doi:10.1029/2001JB000487.
- Dyar, D.M., McEnroe, S.A., Murad, E., Brown, L.L., Schiellerup, H., 2004. The relationship between exsolution and magnetic properties in hemo-ilmenite: insights from Mossbauer spectroscopy. *Geophys. Res. Lett.* 31, L04608, doi:10.1029/2003GL019076.
- Enami, M., Zang, Q.J., Yin, Y.J., 1993. High-pressure eclogites in northern Jiangsu-southern Shandong Province, eastern China. *J. Metamorph. Geol.* 11, 589–603.
- Fountain, D.M., Arculus, R., Kay, R.W., 1992. Continental Lower Crust. Elsevier Science Publisher, pp. 145–178.
- Kasama, T., Golla-Schindler, U., Putnis, A., 2003. High-resolution and energy-filtered TEM of the interface between hematite and ilmenite exsolution lamellae: relevance to the origin of lamellar magnetism. *Am. Mineral.* 88, 1190–1196.
- Kasama, T., McEnroe, S.A., Ozaki, N., Kogure, T., Putnis, A., 2004. Effects of nanoscale exsolution in hematite-ilmenite on the acquisition of stable natural remanent magnetization. *Earth Planet. Sci. Lett.* 224, 461–475.
- Kelso, P.R., Banerjee, S.K., Teyssier, C., 1993. The rock magnetic properties of the Arunta Block, central Australia and their implications for the interpretation of long wavelength magnetic anomalies. *J. Geophys. Res.* 98B, 15987–15999.
- Kletetschka, G., Wasilewski, P.J., Taylor, P.T., 2002. The role of hematite-ilmenite solid solution in the production of magnetic anomalies in ground- and satellite-based data. *Tectonophysics* 347, 167–177.
- Langel, R.A., Hinze, W.J., 1998. The Magnetic Field of the Earth’s Lithosphere: The Satellite Perspective. Cambridge University Press, New York, 429 pp.
- Liou, J.G., Zhang, R.Y., 1996. Occurrence of intergranular coesite in Sulu ultrahigh-P rocks from China: implications for fluid activity during exhumation. *Am. Mineral.* 81, 1217–1221.
- Liu, Q.S., Gao, S., 1992. Geophysical properties of the lower crustal granulites from the Qinling orogenic belt, China. *Tectonophysics* 204, 401–408.

- Liu, Q.S., Gao, S., Liu, Y.S., 2000. Magnetic structure of the continental crustal cross-section in central North China Craton. *J. Geodyn.* 29, 1–13.
- Maher, B.A., 1988. Magnetic properties of some synthetic sub-micron magnetites. *Geophys. J.* 94, 83–96.
- McEnroe, S.A., Langenhorst, F., Robinson, P., Bromiley, G.D., Shaw, C.S.J., 2004. What is magnetic in the lower crust? *Earth Planet. Sci. Lett.* 226, 175–192.
- McEnroe, S.A., Robinson, P., Panish, P.T., 2001. Aeromagnetic anomalies, magnetic petrology and rock magnetism of hemo-ilmenite- and magnetite-rich cumulates from the Sokndal region, South Rogaland, Norway. *Am. Mineral.* 86, 1447–1468.
- Özdemir, Ö., Dunlop, D.J., Moskowitz, B.M., 1993. The effect of oxidation on the Verwey transition in magnetite. *Geophys. Res. Lett.* 20, 1671–1674.
- Özdemir, Ö., Dunlop, D.J., 1999. Low-temperature properties of a single crystal of magnetite oriented along principal magnetic axes. *Earth Planet. Sci. Lett.* 165, 229–239.
- Özdemir, Ö., Dunlop, D.J., Moskowitz, B.M., 2002. Changes in remanence, coercivity and domain state at low temperature in magnetite. *Earth Planet. Sci. Lett.* 194, 343–358.
- Pechersky, D.M., Genshaft, Y.S., 2002. Petromagnetism of the continental crust: A summary of 20th century research. *Phys. Solid Earth* 38, 4–36.
- Pikington, M., Percival, J.A., 2001. Relating crustal magnetization and satellite-altitude magnetic anomalies in the Ungava peninsula, northern Quebec, Canada. *Earth Planet. Sci. Lett.* 194, 127–133.
- Robinson, P., Harrison, R., McEnroe, S., Hargraves, R., 2004. Nature and origin of lamellar magnetism in the hematite–ilmenite series. *Am. Mineral.*, 725–747.
- Robinson, P., Harrison, R., McEnroe, S., Hargraves, R., 2002. Lamellar magnetism in the hematite–ilmenite series as an explanation for strong remanent magnetization. *Nature* 418, 517–520.
- Schlenger, C.M., 1985. Magnetization of the deep crust and the interpretation of regional magnetic anomalies: example from Lofoten and Vestralen, Norway. *J. Geophys. Res.* 90, 11484–11504.
- Toft, P.B., Haggerty, S.E., 1988. Limiting depth of magnetization in cratonic lithosphere. *Geophys. Res. Lett.* 15 (5), 530–533.
- Verwey, E.J., HaaYman, P.W., Romeijn, F.C., 1947. Physical properties and cation arrangement of oxides with spinel structures. *J. Chem. Phys.* 15, 181–189.
- Wang, R.C., Xu, S.J., Xu, S.T., 2000. First occurrence of preiwerkite in the Dabie UHP metamorphic belt. *Chin. Sci. Bull.* 45, 748–750.
- Wasilewski, P.J., Mayhew, M.A., 1992. The Moho as a magnetic boundary revisited. *Geophys. Res. Lett.* 19 (22), 2259–2262.
- Xu, S., Okay, A.I., Ji, S., Sengor, A.M.C., Su, W., Liu, Y., Jiang, L., 1992. Diamond from the Sabie Shan metamorphic rocks and its implication for tectonic setting. *Science* 256, 80–82.
- Xu, H., Jin, Z., Ou, X., Jin, S., Yu, R., 2004. Effects of retrogression of ultrahigh-pressure eclogites on magnetic susceptibility and anisotropy. *Earth Sci. J. China Univ. Geosci.* 29 (6), 674–684 (In Chinese with English abstract).
- Ye, K., Hirajima, T., Ishiwatari, A., Guo, J., Zhai, M., 1996. Significance of interstitial coesite in eclogite at Yangkou, Qingdao City, eastern China. *Chin. Sci. Bull.* 41, 1407–1408.
- Zhang, Z.M., Xu, Z.Q., Xu, H.F., 2000. Petrology of ultrahigh-pressure eclogites from the ZK703 drillhole in the Donghai, eastern China. *Lithos* 52, 35–50.
- Zhang, R.Y., Liou, J.G., Cong, B.L., 1995. Ultrahigh-pressure metamorphism and decompressional *P–T* path of eclogites and country rocks from Weihai, eastern China. *Island Arc* 4, 293–309.